

**Recycling Metal Cutting Chips by Friction Surfacing**

By

Aishwarya Deshpande

A report submitted at the completion of the project supported by the Austrian Marshall Plan  
Foundation Scholarship that was conducted at the IFT, TU Wien

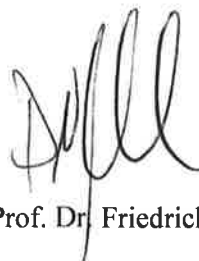
21st May – 21st August 2023

Date of final submission: 16 Nov 2023

The project report is approved by the following members at the home and host university:



Prof. Frank Pfefferkorn, Professor, UW-Madison & Austrian Marshall Plan Foundation endowed  
Professor



University Prof. Dr. Friedrich Bleicher, IFT, TU Wien



Assistant Prof. Stephan Krall, IFT, TU Wien

Title of research project: **Recycling Metal Cutting Chips by Friction Surfacing**

Supervisor at home university: Prof. Frank Pfefferkorn (University of Wisconsin-Madison, USA)

Supervisors at host university: Prof. Friedrich Bleicher, Assistant Prof. Stephan Krall (TU Wien, Austria)

Short description of research agenda:

This work evaluates the feasibility of recycling metal cutting chips by directly using them as feedstock material in the Friction Surfacing process. The objective is to develop an efficient method to recycle metal cutting chips with a reduced environmental impact.

General goals:

- Goal 1:** Study the influence of friction surfacing processing parameters on different objectives when using 304 stainless steel and 6060 aluminum machining chips: e.g., bond strength, consolidation of chips, deposition efficiency - **Completed**
- Goal 2:** Extend the feasibility study by using recycled machining chips of different, commonly-used metal alloys: e.g., medium carbon steel, strain-hardening aluminum - **Completed**
- Goal 3:** Develop a deeper understanding of material flow and temperature evolution during the Friction Surfacing process and how these influence the properties of the deposited material - **Completed**
- Goal 4:** Evaluate energy consumption and embedded energy per volume of material deposited for the Friction Surfacing process: with solid bar stock and recycled machining chips as the feedstock – **Completed**

Summary

To date, recycling metal cutting chips is an energy-intensive process. Researchers are developing methods that can successfully use machining chips as feedstock for additive manufacturing processes. Fullenwider et al. [1], [2] and Jackson et al. [3], [4] propose a mechanical ball milling process to make powder feedstock from machining chips for a fusion-based additive manufacturing process, directed energy deposition. Furthermore, Mahmood et al. [5] and Murray et al. [6] propose the direct use of machining chips in directed energy deposition but commercially available directed energy deposition machines are not yet suitable to adapt such feedstocks. In powder-based additive processes, more work is needed to utilize irregular-shaped feedstocks (such as direct machining chips or mechanically generated feedstocks from machining chips). Compared to fusion-based additive manufacturing processes that meltdown machining chips, solid-state additive processes reduce the overall embodied energy to reuse the chips. Agrawal et al. [7] successfully used recycled Ti-6Al-4V in an additive friction stir deposition process. Tang et al. [8] applied friction extrusion to produce wires from aluminum machining chips. Friction surfacing is one such solid-state process that can potentially reuse metal cutting chips as a feedstock. In friction surfacing, the rotating consumable rod is pressed against the stationary substrate under an applied axial load. The plastically deformed material is traversed over a substrate to deposit a thick, uniform layer. While friction surfacing is primarily used for coating surfaces to improve their wear properties, it is also shown promising results as an additive manufacturing process for repair / remanufacturing features on large metal parts. In this work, we propose consolidating metal cutting chips inside hollow rods and using them as consumable tools in

friction surfacing. Karthik et al.[9] and Gandra et al. [10] used consolidated metal powders in friction surfacing tools to deposit reinforced composite coatings. However, no literature is available that uses machining chips as a feedstock in friction surfacing.

The primary experiments with machining chips of stainless steel 316L and hollow rod 304L have been performed at the proposing university (UW Madison) in collaboration with the host university (TU Wien) in 2022 [11]. The schematic of the process flow can be seen in Figure 1. Results indicate that fully consolidated coatings can be deposited using tools with metal chips consolidated at their core. The primary results of using chip consolidated friction surfacing tools were very insightful but an in-depth study was performed in Summer 2023 in collaboration: proposing university (UW Madison) and host university (TU Wien).

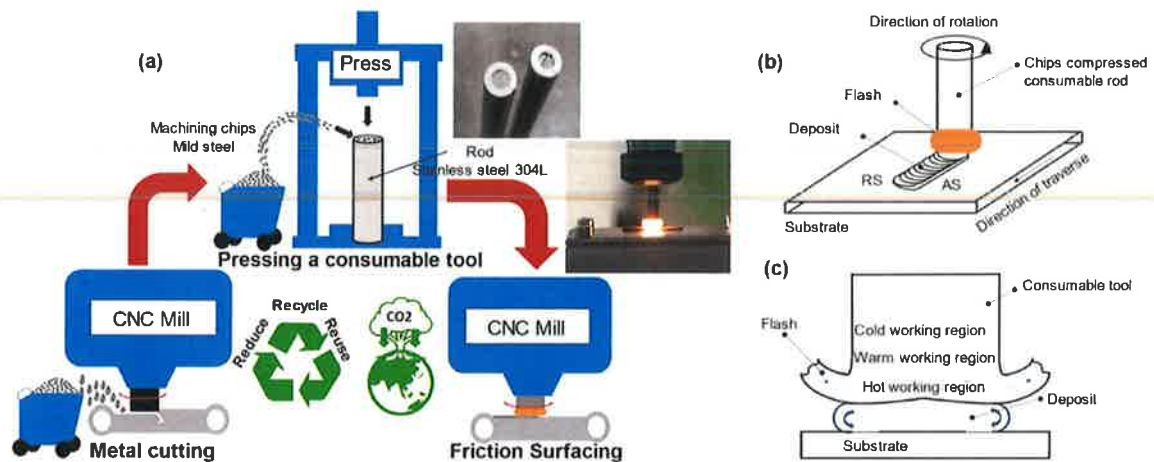


Figure 1: (a) Schematic of process flow (b) Schematic of Friction Surfacing (c) Thermo-Mechanical events of Friction Surfacing

Following people were involved in completing goals of project noted above:

1. Mr. Christian Baumann (doctoral student and researcher at IFT)
2. Assistant Prof. Stephan Krall (IFT)
3. Dipl.-Ing. Dr.techn. Sabine Schwarz (USTEM)
4. Assistant Prof. Thomas Troutner (IFT)

Under the supervision of Prof. Frank Pfefferkorn and Uni. Prof. Friedrich Bleicher.

I am also thankful to following people who helped me during my stay in different ways.

1. Mr. Stephan Kaschnitz-Biegl (IFT)
  2. Severin Maier (IFT)
- And all the IFT staff.

We are preparing 3 publications based on this work, which are presented in the later section of this report. Involved people from the host university and proposing university continue to meet bi-weekly, online, and

work together to analyze and write the results from Summer 2023 as well as continue the research. The work has and will continue to be publicly disseminated through following conferences.

1. 2023 NAMRI/SME North American Manufacturing Research Conference, June 12-17, New Brunswick, NJ, USA
2. 13th International Symposium on Friction Stir Welding, 21 - 23 May 2024, Kyoto, Japan
3. 2024 ASME Manufacturing Science and Engineering Conference, June 17-21, Knoxville, TN, USA

This coming section briefly describes the work that will shortly be published for researchers. Section A covers the work that tries to fundamentally understand machining chips' behavior during the friction surfacing process. Section B covers work that studies energy consumption and the environmental effect of the friction surfacing process. Here are the details of the proposed publications.

1. **Material flow and consolidation behavior of metal cutting chips during friction surfacing**, Aishwarya Deshpande, Christian Baumann, Sabine Schwarz, Stephan Krall, Friedrich Bleicher, Frank E Pfefferkorn
2. **Reusable unit process life cycle inventory for manufacturing: Friction surfacing**, Aishwarya Deshpande, Christian Baumann, Friedrich Bleicher, Barbara Linke, Frank Pfefferkorn

#### **A. Material flow and consolidation behavior of metal cutting chips during friction surfacing**

##### *Abstract*

The objective of this work is to analyze the material flow, and consolidation of the machining chips in friction surfacing process. Metal cutting chips of mild steel 1045 are pressed in stainless steel 304L rods and the rods are then used as consumables in friction surfacing process. The combination of mild steel chips and stainless-steel rod help easily distinguish two materials in the deposit. Although the thermomechanical properties of two materials are different and are relevant for friction surfacing parameter selection, processing regions for two materials were found to be similar. Following conclusions can be made from the results of present work:

- 1 During friction surfacing process, pressed chips gradually compact and complete consolidation of the chips happens only at the tip of the tool where the tool layer finally shears off and form a deposit.
- 2 In friction surfacing process, layer wise deposition can be observed withing single layer where material from the center form a middle and bottom layer while periphery of the rod deposits on the side and top of the deposit.
- 3 Complete consolidation of the chips starts from the plunge stage of the friction surfacing process while different layers of material in the deposit (from center with chips and periphery rod) gradually form in steady state region.

This knowledge can benefit the audience from not only friction surfacing community but also larger community exploring to use machining chips as feedstocks for friction-based processing. High consumption of minerals, generation of energy and production of wastes is a worldwide concern for industrial sector but specifically redlight aluminum and steel industry. Recycling metal cutting chips with low emissions and low energy consumption can help reduce environmental impacts with reduced new metal consumption.

##### *Introduction*

In preliminary work, machining chips of stainless steel 316L were successfully deposited using friction surfacing by pressing in stainless steel 304L hollow rods. Fully consolidated deposits were produced with good bonding with the substrate. Deposits with chip filled rod were thicker and narrower in the morphology compared to solid rod. Plastically deformed layer of machining chips was observed at the bottom of the friction surfacing tool. In depth discussion on morphology, deposition efficiency, and process

forces was presented in this publication [11]. However, how chips material flow and plastically deform in the friction surfacing process from the compressed and non-sintered in the rod to fully consolidated deposit during the process was not fully understood. This work investigates the material flow of the chips material in friction surfacing process. A very few literatures have attempted to understand material flow in the friction surfacing process. Karthik et. al. and Gandra et. al. [9], [10] introduced re-enforcement powder in the friction surfacing rod to deposit titanium reinforced Aluminum and SiC-Aluminum composites respectively. Composites were successfully deposited with variation in the particle densities in the deposit by varying locations and number of holes in the consumable rod. The common observation in these studies was that there was more powder density in the deposit when powder pressed holes were closer to the center of rod while powder density in the deposit reduced when holes were away from the center. This suggests that the material from the center of the rod flows to the deposit while outer periphery material rolls out to form a flash. Fukakusa studied material flow in the friction surfacing and friction welding process [12], [13] with tracer rod pressed at the center and found a similar trend where central material of the rod was deposited while outer periphery material was found in the flash. Fukakusa defines this central part as ‘real rotational contact plane’ through which material actually flows to the substrate forming a deposit. The same phenomenon of real rotational contact plane was observed in friction welding process. Friction welding is a solid-state process where rotating rod is plunged into the substrate to weld the rod to the substrate. The knowledge of friction welding process is relevant because friction surfacing initially starts by plunging into the substrate just like friction welding. Rafi et al.[14] also studied material flow in friction surfacing with X-ray radiography by introducing tungsten powder as a marker in stainless steel rod. Results found that material flows from the advancing side (direction of rotation of consumable tool and traverse are same) to the retreating side (direction of rotation of consumable tool and traverse are opposite) of the deposit terminating at the center during friction surfacing. In the deposit, two layers could be distinguished based on material flow, top layer dominated by tool rotational movement while the bottom layer material flow is governed by traverse (linear) motion of the substrate with respect to rotating spindle. All these works greatly explain the events of the friction surfacing process qualitatively mostly with solid rods and some trace amounts of powders, as summarized in the Figure 2.

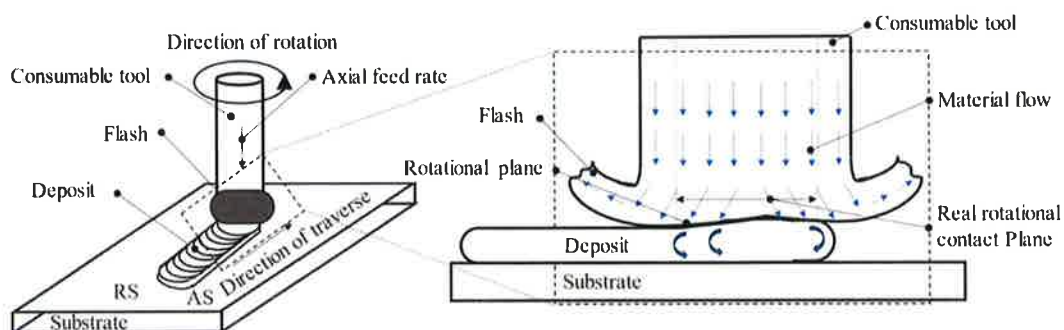


Figure 2: Schematic of friction surfacing with material flow model with literature

In present work, machining chips pressed in the hollow rod are not fully dense (~70-80 %) and fed relatively in high amounts in the rod (hole dia/ rod dia > 0.5). However, fundamental knowledge of consolidation behavior of chips and its evolution into fully dense deposit is not fully explored in the literature. T. Peng et. al. [13] studied consolidation behavior of Mg-10Gd-2Y-0.5Zr chips during conventional extrusion and cyclic extrusion compression. It is noted that an essential factor for recycling of chips in extrusion is the destruction of oxide layer by severe plastic deformation. Shear plastic

deformation further promotes atom diffusion at elevated temperatures which successfully consolidates the machining chips in solid-state extrusion recycling process. Unlike extrusion, friction surfacing as well as additive friction stir deposition processes involve complex interaction of heat generation through friction and plastic deformation, tool rotation plus traverse movement and applied pressure. Hence it is essential to investigate chips consolidation behavior for friction based solid state processes.

The objective of this work is to thoroughly investigate how chips material pressed in hollow rod consolidate and flow in the fully dense deposit in the friction surfacing process. Fundamental questions are how and where chips deposit vs hollow consumable rod, and when and how pressed chips consolidate the hollow consumable tool.

#### *Experimental Set up*

Metal cutting chips of mild steel 1045 from a milling operation were consolidated inside hollow 304L stainless steel rods ( $D_o$ ) of 10 mm diameter and hole diameters ( $D_i$ ) of 3, 4, 5, 6. Chips of uniform size and shape were produced without use of any coolant. The consolidated chips rods were used as consumable feedstocks in friction surfacing. The substrates were 5 mm thick stainless steel 304L plates. All friction surfacing experiments were conducted on a three-axis CNC mill (HAAS VF1) at a constant plunge rate of 20 mm/min, spindle rotation speed of 4000 RPM and traverse feed rate ( $V_x$ ) of 139.27 mm/min. The axial feed rate ( $V_z$ ) was appropriately chosen to keep a constant velocity ratio ( $V_z/V_x$ ) of 0.4. To understand the development of deposit and consolidation of chips over the events of friction surfacing, four deposits were made with each chip filled hole diameter. Firstly, the tool was only plunged onto the substrate, dwelled for 25 microseconds and retracted while spindle rotation on. For the next samples, the process was continued for 3 mm, 5 mm and, 30 mm traverse distance each. Table 1 summarizes the tool dimensions and process parameters applied for the friction surfacing experiments. The substrate was mounted atop a three-axis piezoelectric force dynamometer (Kistler model 9285), which measured the transient process forces.

Tables 1: Process parameters table

Tool diameters ( $D_o$ )	10 mm
Hole diameters ( $D_i$ )	3, 4, 5, 6 mm
Spindle speed (N)	4000 rpm
Feed rate ( $V_x$ )	139.27 mm/min
Velocity ratio ( $V_z/V_x$ )	0.4 []
Plunge rate ( $V_p$ )	20 mm/min
Plunge depth ( $D_p$ )	1 mm
Deposition length (L)	0 (only plunge and dwell), 3, 5, 30 mm

Deposits were then cross sectioned along and perpendicular to the direction of deposit and friction surfacing rods were cross-sectioned in the center. Samples were mounted in conductive media then grinded and polished sequentially with 240 sandpaper, 9  $\mu$ m, 3  $\mu$ m, 1  $\mu$ m and 5 nm colloidal solution. Deposition morphology, i.e., total width (W), bonded width (B) and thickness (T) were analyzed using a white light optical metrology system ( Alicona, InfiniteFocus® G4, Austria). Samples were etched in Nital solution at room temperature for 12 seconds. Due to high chromium content in the stainless steel, it does not etch under

applied conditions while mild steel etches, and microstructure can be observed. Etched samples were then imaged using the white light optical metrology system. SEM (Scanning electron microscope) was used for high resolution imaging. EDX (Energy-dispersive X-ray spectroscopy) method is used to validate the etching results by differentiating two materials by elemental difference. EDX analysis is also used to analyze oxide layers (i.e. consolidation level) on the chips in friction surfacing rods. Although EDX is not an effective technique to quantitatively measure the lighter elements like oxygen, EDX maps can show relative concentration of oxygen level at different positions qualitatively. Lamellae was then cut out from the rod at different locations to perform TEM analysis.

### *Result and Discussion*

Fully consolidated deposits were obtained with mild steel machining chips pressed in stainless steel 304L hollow rods. As found in earlier study with stainless steel 316L chips, the deposit produced with chip filled tool is thicker and narrower than deposit produced with solid rod. This suggests that the behavior of the mild steel chips is very similar with stainless steel 316L chips.

#### a. Friction surfacing tool after deposition

Various layers can be distinguished in the friction surfaced tools based on compaction level of chips along the depth. Towards the tip of the tool, a fully consolidated thin layer was observed. This layer is comparatively thin (~1-2 mm). Homogeneous microstructure can be observed in this region with typical ferritic and pearlitic microstructure. The temperature at the tool interface is expected to go up to 70-80% melting temperature of steel which is above the austenitic temperature of mild steel. Figure 3 iii shows the image from the area in a well compacted layer. Distinct boundary lines can be observed which could result from inhomogeneities or oxide layers on the chips' surfaces. This suggests that chips are compressed but not fully consolidated in this region. Figure 3 iv shows EDX analysis around such boundaries. High concentration of oxygen on the boundaries supports the existence of oxides layer. Hence, no diffusion bond has been formed between the chips in this layer. The layer above the well compacted layer is loosely compacted chips as gaps between the chips can be clearly seen. Packing density of the chips in this area must not have significantly changed from as 'pressed' conditions. These three regions of chips in the friction surfacing tool suggest that chips are gradually compressing and consolidating during friction surfacing as the process goes on. Gandra et al. [15] explained thermomechanical events happening during friction surfacing with solid rod. Under axial feed with rotational and lateral movement, rubbing interface is formed near the tool tip followed by hot, warm and cold working region. Different compaction levels of the chips can be correlated to this thermal evolution of the tool. This suggests that the chip filled tool above behaves same as solid rod. As fully consolidated layer is very small, complete plastic deformation of the chips must be happening when chips enter rubbing interface. Before entering the rubbing interface, chips gradually compress under localized pressure and temperature.

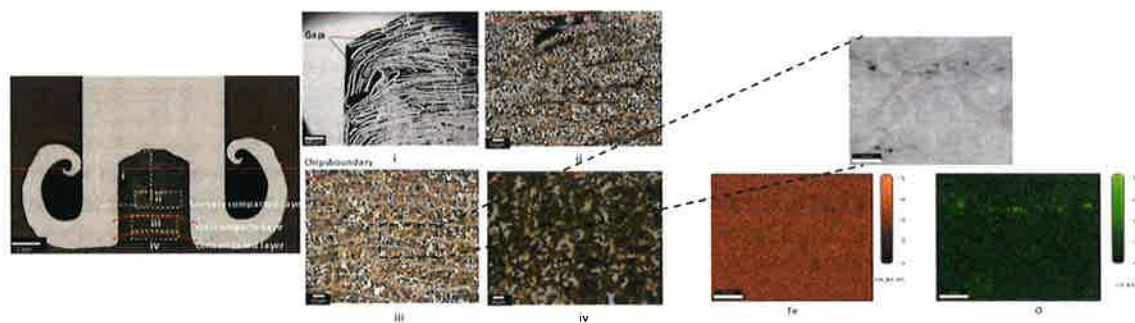




Figure 3: Images of Consumable rod after deposition at different locations i.,ii. SEM and Optical image of area in loosely compacted chips layer iii. Optical image of area in well compacted layer iv. Optical image of area in consolidated layer v. Elemental analysis of area in well compacted layer with visible oxygen concentration between the chips

b. Friction surfacing Deposit

In the fully consolidated deposit as shown in Figure 4, two distinct layers of mild steel and stainless steel can be distinguished after etching. Figure 3 is a cross-section of deposit with a 5 mm hole diameter rod. Two separate layers suggest the layer-wise deposition behavior of friction surfacing process where material at the center gets deposited in the middle and the bottom of the deposit while outer periphery rod material deposits around and above it. EDX analysis was performed to validate the material identification. Higher chromium and nickel concentration in the top layer confirms that it indeed is a stainless-steel layer. Next section explains role of hole diameter on the material flow behavior in the deposit. The fine grain microstructure of the mild steel in the deposits is ferritic and pearlitic with some traces of martensite. For the deposited layer, substrate provides a heat sink which results in faster cooling rates. Fine grains of are observed in the deposit which are typically observed in friction surfacing deposits due to dynamic recrystallization imposed under hot working conditions. This suggests that it is feasible to utilize friction surfacing to re-use machining chips as a feedstock. A well-consolidated layer with a typical fine microstructure can be deposited for various applications.

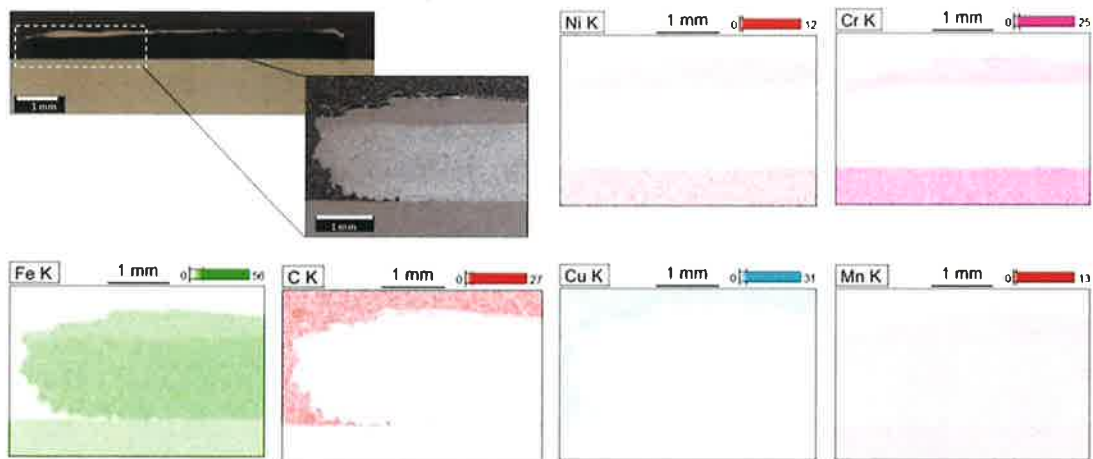


Figure 4: EDX map of Deposit's region

c. Consolidation behavior of chips

Chips inherently carry inhomogeneities and oxide layers formed on the surface. The question is what happens to these oxide layer during and after the friction surfacing process. TEM analysis was performed to investigate this phenomenon closely. Lamella was cut in consolidated region of the chips in the tool. Chemical analysis showed that manganese oxide granulates are present in the consolidated region of the chips. Further investigation is in process to validate the results.

d. Material flow dependence on hole diameter/Estimating real rotational contact plane.

As mentioned in earlier section, friction surfacing process follow a layer wise deposition with center of the tool (in this case chips) deposits in the middle and bottom of the deposit while outer periphery of the tool deposits on the side and top layer of the deposit. This behavior can be clearly observed with deposits from tool of different chip filled hole diameter. With increasing the hole diameter of chips, more chips material vs tool material can be observed in the deposit. Note that the packing density of the chips in the rods was not identical. In the deposit with 3mm hole diameter, chips material can be observed in the middle surrounded by the stainless steel. With increasing hole diameter, the stainless-steel amount reduces and shallow down only to top layer. For higher hole diameter rod deposit, the deposit is only chips material and stainless-steel rod flow out in the flash. These results agree with the observations noted by Fukakusa [12], Karthik et al.[9] and Gandra et. al. [10]. Material from the center of the rod deposits while the material from outer periphery flows out in the flash. Fukakusa developed the methodology to calculate the radius of the real rotational contact plane for solid rods using weight of the deposited layer and the consumed rod. In the chips filled rod case, packing density of the chips plays an important role. The exact calculations of radius of real rotational contact plane are not possible as both chips anulus with low density and the outer solid rod get deposited. But we propose to calculate a range of real rotational contact plane which provide a predictive tool to estimate whether chips or shell material or both will get deposited. Max radius of contact value corresponds to a case where whole rod is only pressed chips while minimum value considers the entire rod to be solid. The calculated range match the results as rods with hole diameters from 3 mm to 5 mm have radius of real rotational contact plane is higher than the hole diameter. While for 6 mm hole diameter, radius of real rotational contact plane is less than 6 mm.

$$r_{c\_max} = \sqrt{\frac{W}{\Pi\rho_{chips}a}}$$

$$r_{c\_min} = \sqrt{\frac{W}{\Pi\rho_{rod}a}}$$

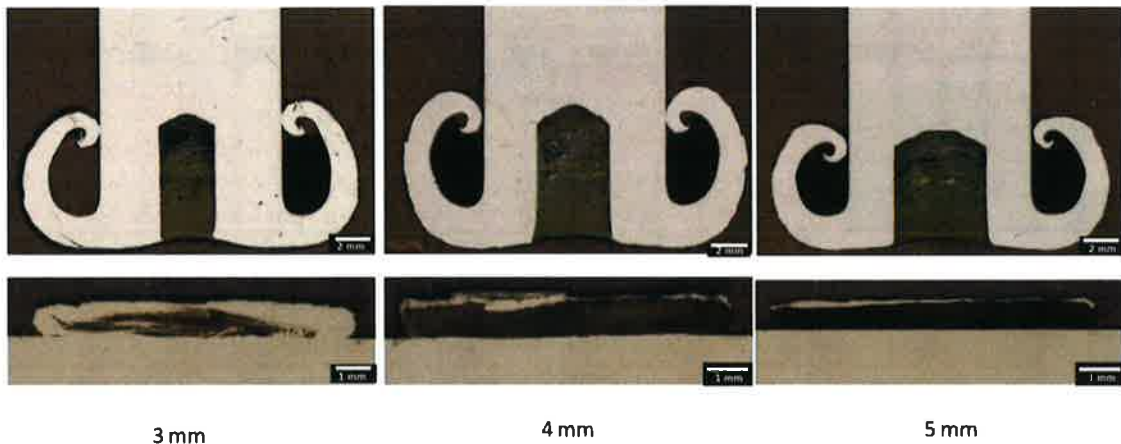


Figure 5: Images of a. cross section of rod and deposit when just plunged b. cross section of rod and deposit 3

e. Progression of plastically deformed layer from preheating to steady state

To understand how deposit is developed during the friction surfacing process, operation was interrupted at various stages during the deposition to understand progression of friction surfacing process with the chip filled rod. Figure shows cross sections of deposits along the direction of deposits of just a plunge, plunge plus 5mm traverse and a 30mm traverse with 5mm hole diameter. The tool was retracted back after the respective deposition with spindle rotation on. In the plunge, the morphology of the deposit is same as the profile of the rod with chips in the middle. Even in the plunged tool, a small flash is visible around the rod. Although chips were not fully dense in the rod when the process began, the chips in the deposit were fully solid. A small fully consolidated layer is visible in the rod which suggest the chips have started to plastically deform even in the plunge. As the process progressed, after 5 mm traverse, a small layer of mild steel at the top of the deposit has started to develop is visible but process does not seem steady-state. If we look at the cross section with 30 mm traverse, chips layer is settled down with a small layer of stainless steel on the top of the deposit. Two major conclusions can be made in this work is that total radius of contact is gradually formed from plunge to steady state region. And material is pushed from the back of the tool as stainless steel layer (ie. periphery rod material) is observed in the top of the deposit.

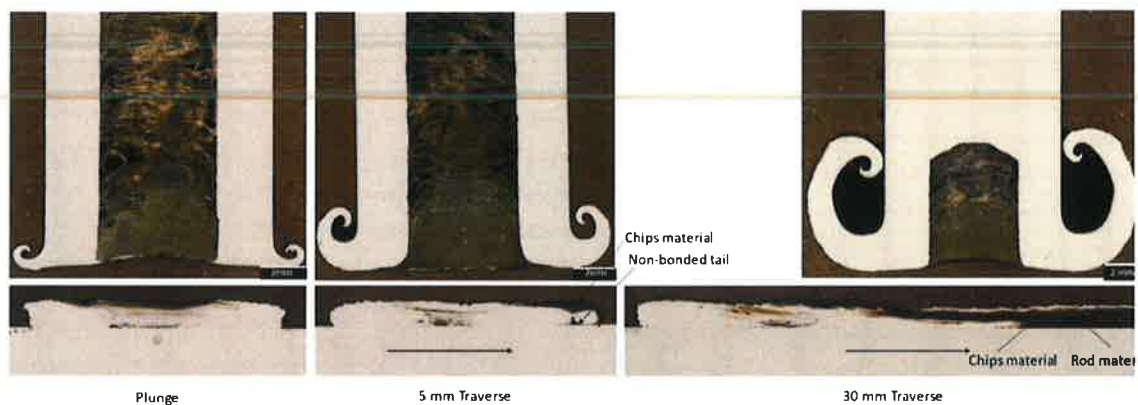


Figure 6: Images of a. cross section of rod and deposit when just plunged b. cross section of rod and deposit 5 mm traverse c. cross section of rod and deposit 30 mm traverse

### Conclusion

In this work, material flow, and consolidation of the machining chips in friction surfacing process was studied by pressing mild steel 1045 chips in hollow stainless-steel rod. The hole diameter in the rod was varied to understand the behavior of the process. Also, process was interrupted in between understand the progression of the process. Following outcomes were learned:

- 1 During friction surfacing process, pressed chips gradually compact and complete consolidation of the chips happens only at the tip of the tool where the tool layer finally shears off and form a deposit.
- 2 In friction surfacing process, layer wise deposition can be observed withing single layer where material from the center form a middle and bottom layer while periphery of the rod deposits on the side and top of the deposit.
- 3 Complete consolidation of the chips starts from the plunge stage of the friction surfacing process while different layers of material in the deposit (from center with chips and periphery rod) gradually form in steady state region.

The results suggest that machining chips can be potentially used as a feedstock in solid state additive manufacturing processes such as friction surfacing. And the process dynamics is capable of fully consolidating the chips material by destroying the oxide/inhomogeneous layers on the chips.

## B. Reusable unit process life cycle inventory for manufacturing: Friction surfacing

### Abstract

Objective of this work is to provide users with calculation tools to estimate the energy use and mass loss of one unit process in a full manufacturing line. It is known as a unit process life cycle inventory (UPLCI). This paper discusses friction surfacing process's energy consumption and environmental effects applying UPLCI approach. The friction surfacing process falls under solid-state friction-based deposition process where frictional heat and heat generated due to plastic deformation of consumed material is used for depositing the material and no external heat source is required for processing. In this work a basic energy consumption model has been developed assuming process's general sequence for one layer deposition. Energy consumption value is calculated for one condition. The work is in process to add more data in the analysis.

### Introduction

Friction surfacing process is primarily studied and applied as a coating technology to apply wear resistant and corrosion resistant layer for high temperature corrosion prone applications [16]. Lately, it is also been considered as potential additive manufacturing process [17], [18] to repair/ remanufacture damaged parts and to manufacture large parts. Solid-state nature of the process makes it attractive to produce parts with reduced energy consumption and CO<sub>2</sub> emissions than fusion based additive manufacturing processes. Although this process is at its developing stage and not currently applied as a mass production technology, UPLCI guidelines can parallelly provide researchers, practitioners, and policy makers with a tool to examine friction surfacing process for energy consumption and environmental impacts. Process schematic and thermomechanical characteristics of the friction surfacing process can be seen in Figure 1. From a thermomechanical standpoint, consumable tool goes from cold to hot working region before it deposits as a successive layer of material. Applied torque, applied pressure and heat generated during the process produce signature deposit bonded to the substrate.

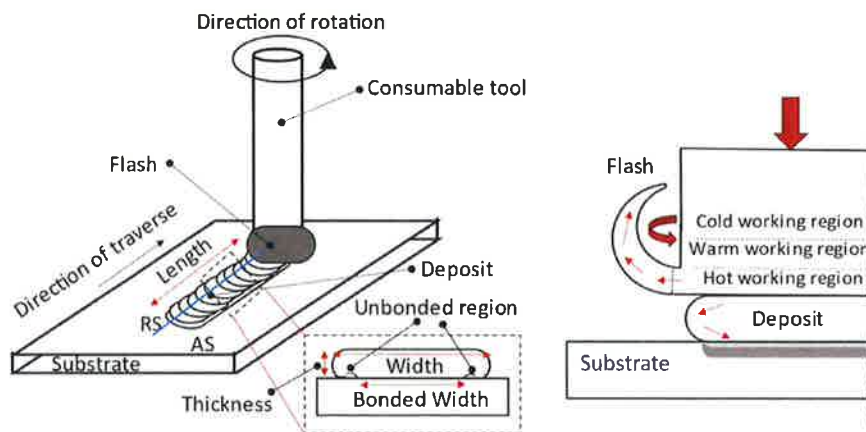


Figure 7: a. Process schematic (General) b. Thermo-mechanical events occurring during friction surfacing  
 2. Schematic involving morphology dimensions and process parameters (Make A-A line for cross section)

Solid state nature of the process makes the deposit free of fusion based defects such as porosities and cracking. And deposits generally develop fine microstructure from dynamic recrystallization which exhibit better mechanical properties than additive fusion-based processes. Two methods are widely applied to implement the friction surfacing process. First is a force control method where special purpose machines (e.g., friction stir processing machine) maintain specified force over the rotating consumable rod material during deposition. Alternative approach is feed-rate control method which can be implemented on any CNC milling set up where axial feed-rate is maintained over the consumable tool during the deposition process. Both have been successfully implemented, although the force control method is more convenient with known hot working conditions. Feed rate is noted to be related to force during the deposition conditions, hence any user with access to position-controlled CNC milling set up can implement friction surfacing process. Generally speaking, most milling machines are capable of being hybrid machines as they are capable of implementing additive (ie., friction surfacing) and subtractive both on the same set up. This work applies feed control method friction surfacing experiments with 3-axis CNC machine HAAS VF2.

Objective of this work is to provide re-usable UPLCI tool to estimate energy consumption and environmental impacts of friction surfacing process. Researchers, practitioners and policy makers can refer to this tool to get insights for various potential friction surfacing applications.

*Methodology for unit process life cycle inventory model*

To thoroughly assess energy consumption and environmental impact of friction surfacing with reusable model, the concept of unit operation is considered. Unit operation means the input, process and the output of that operation. Figure 8 represents the unit operation diagram of the friction surfacing process. As represented, input for the process is material (substrate, consumable rod, etc), energy and other things like shielding gases etc. depending on the application. Some of the materials are re-usable in the process as indicated by the separate output channel while some is wasted in the form of flash or unbonded edges of the deposit which are undesirable but unavoidable for the unit friction surfacing process. Energy is input into the system in different forms like thermal, compressed air, electrical energy. But this work estimates energy consumed in the form of electricity and not others because they do not explicitly enter the process from controlled channel.

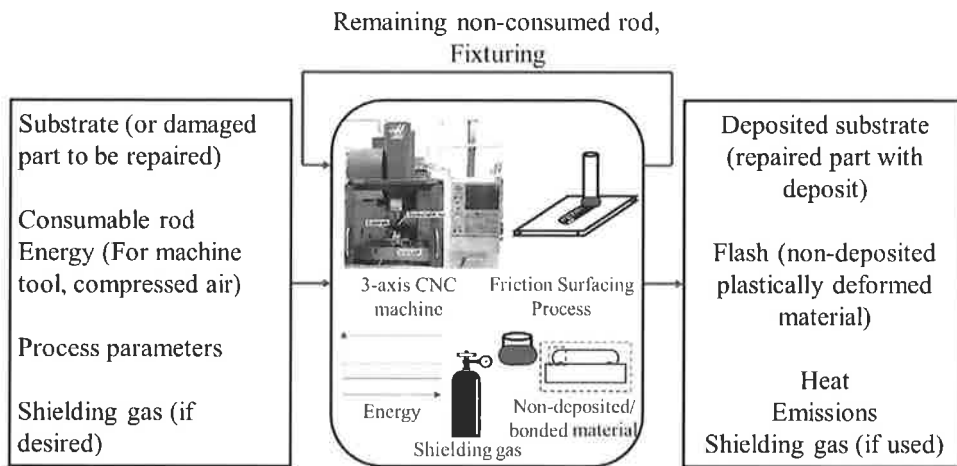


Figure 8: Input-Output diagram of a friction surfacing process

### Process characteristics

For generalized case, following sequence is considered for the UPLCI model for friction surfacing.

1. Machine start up routine is excluded from the model. This particular study considers 3 axis CNC machine as a tool to perform the friction surfacing process.
2. The generalized model is designed for single layer deposition, but adjusted model is provided for multi-layer or multi-track depositions.
3. *Basic time ( $t_{basic}$ ) and power ( $P_{basic}$ ):* the overall cycle time (part in to part out) is used for basic energy calculations. It includes the process set up, loading and unloading of substrate and the tool. Loading and unloading are in the range of 10–60 s depending on the size of the parts and the process set-up. Process set up time can be machine turn on, turn off routine is excluded in the basic time as it is generally done once in a day. As seen from Fig. 4, the basic power is constant over the cycle time and typically includes basic machine tool motors, Air suction, oil pumps (if any), machine lighting, Numerical control.
4. *Idle time ( $t_{idle}$ ) and Power ( $P_{idle}$ ):* Idle power/time is required for any tasks during the process cycle that is required before or after the actual deposition, as shown in Fig. 4. In friction surfacing, spindle and machine bed's over travel when tool is approaching and retracting from the substrate is included in the total idle time. The idle power  $P_{idle}$  is the W above basic power, Fig. 4.
5. *Friction Surfacing time ( $t_{FS}$ ) and Power ( $P_{FS}$ ):* It is the actual time when the consumable rod touches the substrate, and the deposit the material. It is basically a power to plastically deform the consumable rod and bond it to a substrate. Friction Surfacing power  $P_{FS}$  is the W above that measured during idle, Fig. 4.
6. *Total energy ( $E_{total}$ ):* It is calculated by measuring area under the overall power consumed curve for the respective time (as shown in Fig 4).

$$E_{total} = P_{basic} \times (t_{basic}) + P_{idle} \times (t_{idle}) + P_{FS} \times (t_{FS}) = \text{Basic energy} + \text{Idle energy} + \text{Friction Surfacing energy}$$

7. In the case of multi-layer or multi-track friction surfacing applications, *Total energy ( $E_{total}$ )* consumption can be approximated by incorporating a number of tool changes in between

$$E_{total} = n_{basic} \times P_{basic} \times (t_{basic}) + n_{idle} \times P_{idle} \times (t_{idle}) + P_{FS} \times (t_{FS})$$

Here,  $n_{basic}$  and  $n_{idle}$  are tool change factors associated with basic time and idle time respectively. For single layer deposition  $n_{basic}$ ,  $n_{idle}$  are unity. More details on this are provided in later section.

8. Plunge peak is avoided in the calculation of as plunge takes less than 10% of total deposition time. However, if plunge is not instantaneous, then one will have to add energy consumption in the friction surfacing power.

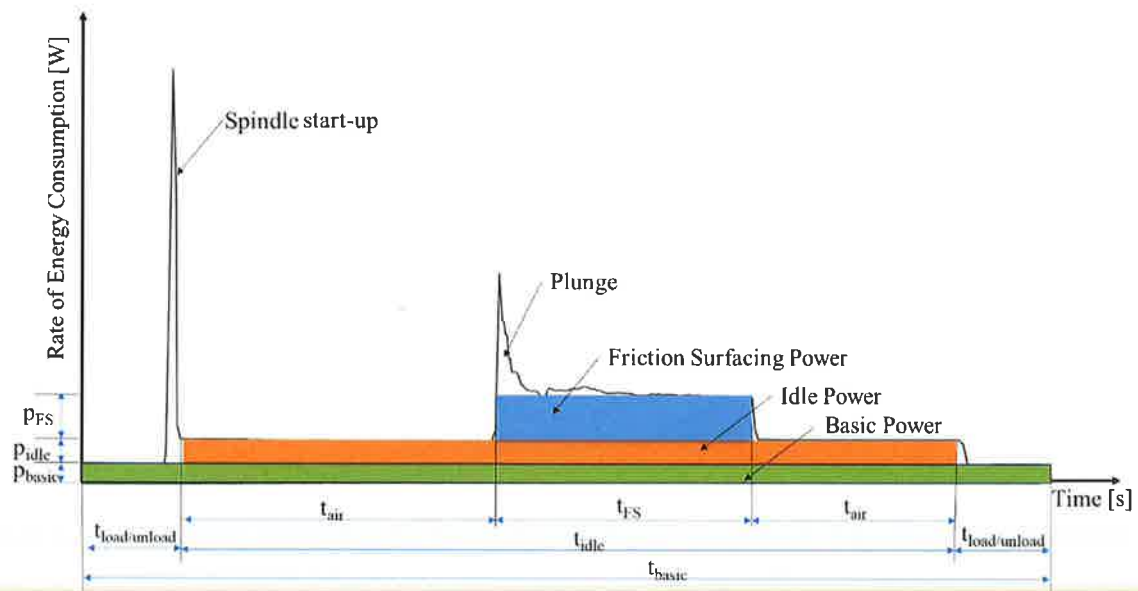


Figure 9: Generic electric power and time profile in friction surfacing with energy as the area under the power–time graphs

#### Case study

Energy consumption is calculated for following set of process parameters:

Tool diameters ( $D_o$ )	10 mm
Spindle speed (N)	4000 rpm
Feed rate ( $V_x$ )	139.27 mm/min
Velocity ratio ( $V_z/V_x$ )	0.4 []
Plunge rate ( $V_p$ )	20 mm/min
Plunge depth ( $D_p$ )	1 mm
Deposition length (L)	30 mm

Time calculation for the case study

#### Friction surfacing time

$$t_{FS} = L / V_x + L_p / V_p = 30 / 150 + 1 / 20 = 15 \text{ sec}$$

#### Idle time

$$t_{idle} = t_{FS} + t_{air} = 50 \text{ sec}$$

$$t_{air} = \text{Home position to zero position} + \text{Approach/overtravel times} + \text{retraction times}$$

#### Basic time

$$t_{\text{basic}} = t_{\text{idle}} + t_{\text{load/unload}} = 125 \text{ sec}$$

$t_{\text{load/unload}}$  = load/unload substrate and consumable tool

From the collected data, following power values were observed

$$P_{\text{FS}} = 1500 \text{ W}; P_{\text{idle}} = 735 \text{ W}; P_{\text{basic}} = 565 \text{ W};$$

$$\text{Total energy consumption } E_{\text{total}} = P_{\text{basic}} \times (t_{\text{basic}}) + P_{\text{idle}} \times (t_{\text{idle}}) + P_{\text{FS}} \times (t_{\text{FS}}) = 1500 \times 15 + 735 \times 50 + 125 \times 535 = 22500 + 36850 + 66875 = 126225 \text{ J} = 126.225 \text{ KJ}$$

For the 30 mm long deposit, 126.225 KJ energy get consumed. We can observe that the deposition energy consumption is comparatively lower than basic and idle consumption of the machine. As the deposition length would increase, the contribution of basic and idle energy consumption would decrease.

*Parameters affecting energy required for Friction surfacing process*

Friction surfacing energy consumption ( $E_{\text{FS}}$ ) can basically be looked at as energy required to plastically deform the consumable material. And a set of process parameters, tool geometry and material in friction surfacing mainly affect plastic deformation of the material and effectively energy consumption.

In this project, effect of following process parameters are studied.

1. Spindle speed (N)
2. Traverse feed rate ( $V_x$ )
3. Axial feed rate ( $V_z$ )
4. Consumable tool material
5. Consumable tool diameter

Data analysis is in process and will be presented in publication coming soon on the topic.

*Process losses*

From the following formulae, Deposition efficiency of the process can be calculated.

Material consumption rate:

$$\text{Material consumption rate} = \frac{\pi}{4} \cdot D^2 \cdot \rho \cdot V_z$$

Deposition Rate:

$$\text{Deposition rate} = W \cdot T \cdot V_x \cdot \rho$$

Deposition Efficiency

$$\text{Deposition efficiency} = \frac{\text{Deposition rate}}{\text{Material Consumption Rate}}$$

By taking process losses into account ~ 20% energy is used for depositing the material while rest is lost in the process losses. More details on the topic will be presented in the upcoming publication.

*Conclusion*



In this work, energy consumption model of friction surfacing process using UPLCI model approach has been developed. A test result for sample conditions are presented. More detailed work is in process where effect of process conditions, materials etc. is been investigated.

#### References

- [1] B. Fullenwider, P. Kiani, J. M. Schoenung, and K. Ma, "Two-stage ball milling of recycled machining chips to create an alternative feedstock powder for metal additive manufacturing," *Powder Technology*, vol. 342, pp. 562–571, Jan. 2019, doi: 10.1016/j.powtec.2018.10.023.
- [2] B. Fullenwider, P. Kiani, J. M. Schoenung, and K. Ma, "From Recycled Machining Waste to Useful Powders for Metal Additive Manufacturing," in *REWAS 2019*, G. Gaustad, C. Fleuriault, M. Gökelma, J. A. Howarter, R. Kirchain, K. Ma, C. Meskers, N. R. Neelameggham, E. Olivetti, A. C. Powell, F. Tesfaye, D. Verhulst, and M. Zhang, Eds., in *The Minerals, Metals & Materials Series*. Cham: Springer International Publishing, 2019, pp. 3–7. doi: 10.1007/978-3-030-10386-6\_1.
- [3] M. A. Jackson, A. Kim, J. A. Manders, D. J. Thoma, and F. E. Pfefferkorn, "Production of mechanically-generated 316L stainless steel feedstock and its performance in directed energy deposition processing as compared to gas-atomized powder," *CIRP Journal of Manufacturing Science and Technology*, vol. 31, pp. 233–243, Nov. 2020, doi: 10.1016/j.cirpj.2020.05.014.
- [4] M. A. Jackson, J. D. Morrow, D. J. Thoma, and F. E. Pfefferkorn, "A comparison of 316 L stainless steel parts manufactured by directed energy deposition using gas-atomized and mechanically-generated feedstock," *CIRP Annals*, vol. 69, no. 1, pp. 165–168, Jan. 2020, doi: 10.1016/j.cirp.2020.04.042.
- [5] K. Mahmood, A. Khan, and A. Pinkerton, "Laser Metal Deposition of Steel Components using Machining Waste as Build Material," in *CLEO:2011 - Laser Applications to Photonic Applications (2011)*, paper JTuh5, Optical Society of America, May 2011, p. JTuh5. doi: 10.1364/CLEO\_AT.2011.JTuH5.
- [6] J. W. Murray, A. Speidel, A. Jackson-Crisp, P. H. Smith, H. Constantin, and A. T. Clare, "Unprocessed machining chips as a practical feedstock in directed energy deposition," *International Journal of Machine Tools and Manufacture*, vol. 169, p. 103803, Oct. 2021, doi: 10.1016/j.ijmachtools.2021.103803.
- [7] P. Agrawal *et al.*, "Processing-structure-property correlation in additive friction stir deposited Ti-6Al-4V alloy from recycled metal chips," *Additive Manufacturing*, vol. 47, p. 102259, Nov. 2021, doi: 10.1016/j.addma.2021.102259.
- [8] W. Tang and A. P. Reynolds, "Production of wire via friction extrusion of aluminum alloy machining chips," *Journal of Materials Processing Technology*, vol. 210, no. 15, pp. 2231–2237, Nov. 2010, doi: 10.1016/j.jmatprotec.2010.08.010.
- [9] G. M. Karthik, G. D. J. Ram, and R. S. Kottada, "Friction deposition of titanium particle reinforced aluminum matrix composites," *Materials Science and Engineering: A*, vol. 653, pp. 71–83, Jan. 2016, doi: 10.1016/j.msea.2015.12.005.
- [10] J. Gandra, P. Vigarinho, D. Pereira, R. M. Miranda, A. Velhinho, and P. Vilaça, "Wear characterization of functionally graded Al–SiC composite coatings produced by Friction Surfacing," *Materials & Design (1980-2015)*, vol. 52, pp. 373–383, Dec. 2013, doi: 10.1016/j.matdes.2013.05.059.
- [11] A. Deshpande, H. Agiwal, C. Baumann, S. Krall, F. Bleicher, and F. E. Pfefferkorn, "Recycling metal cutting chips into a consolidated deposition with friction surfacing," *Manufacturing Letters*, vol. 35, pp. 743–749, Aug. 2023, doi: 10.1016/j.mfglet.2023.08.093.
- [12] K. Fukakusa, "On the characteristics of the rotational contact plane - a fundamental study of friction surfacing," *Welding International*, vol. 10, no. 7, pp. 524–529, Jan. 1996, doi: 10.1080/09507119609549043.

- [13] K. Fukakusa, "Real rotational contact plane in friction welding of different diameter materials and dissimilar materials: Fundamental study of friction welding," *Welding International*, vol. 11, no. 6, pp. 425–431, Jan. 1997, doi: 10.1080/09507119709451991.
- [14] H. Rafi, G. Phanikumar, and P. Kalvala, "Material Flow Visualization during Friction Surfacing," *Metallurgical and Materials Transactions A-physical Metallurgy and Materials Science - METALL MATER TRANS A*, vol. 42, pp. 937–939, Apr. 2011, doi: 10.1007/s11661-011-0614-2.
- [15] J. Gandra, R. M. Miranda, and P. Vilaça, "Performance analysis of friction surfacing," *Journal of Materials Processing Technology*, vol. 212, no. 8, pp. 1676–1686, Aug. 2012, doi: 10.1016/j.jmatprotec.2012.03.013.
- [16] H. Agiwal, H. Yeom, K. A. Ross, K. Sridharan, and F. E. Pfefferkorn, "Leak-tight crack repair for 304L stainless steel using friction surfacing," *Journal of Manufacturing Processes*, vol. 79, pp. 532–543, Jul. 2022, doi: 10.1016/j.jmapro.2022.05.004.
- [17] S. Krall, C. Baumann, H. Agiwal, F. Bleicher, and F. Pfefferkorn, "Investigation of Multilayer Coating of EN AW 6060 - T66 using Friction Surfacing," *Journal of Machine Engineering*, vol. 22, no. 3, pp. 44–58, Mar. 2022, doi: 10.36897/jme/147502.
- [18] M. Soujon, Z. Kallien, A. Roos, B. Zeller-Plumhoff, and B. Klusemann, "Fundamental study of multi-track friction surfacing deposits for dissimilar aluminum alloys with application to additive manufacturing," *Materials & Design*, vol. 219, p. 110786, Jul. 2022, doi: 10.1016/j.matdes.2022.110786.